



# Fine structure splitting of isoelectronic bound excitons in nitrogen-doped GaAs

Kita, Takashi  
Harada, Yukihiro  
Wada, Osamu

---

(Citation)

Physical Review B, 77(19):193102-193102

(Issue Date)

2008-05

(Resource Type)

journal article

(Version)

Version of Record

(URL)

<https://hdl.handle.net/20.500.14094/90000580>



# Fine structure splitting of isoelectronic bound excitons in nitrogen-doped GaAs

Takashi Kita,\* Yukihiro Harada, and Osamu Wada

Department of Electrical and Electronics Engineering, Graduate School of Engineering, Kobe University, Rokkodai 1-1, Nada, Kobe 657-8501, Japan

(Received 3 April 2008; published 5 May 2008)

We have studied the fine structure polarization splitting of exciton emission lines related to isoelectronic centers in an nitrogen-doped GaAs. The nitrogen doping has been performed in atomically controlled way using the  $(3 \times 3)$  nitrogen stable surface of GaAs(001), which forms a series of distinct, strong, narrow bandwidth luminescence lines. The localized bound excitons have been found to consist of four signals, which can be selected by linear polarization. Magnetic-field-induced change in the splitting shows a quadratic dependence of the bright exciton splitting owing to the in-plane Zeeman interaction. Our calculations of the optical selection characteristics considering both the  $J$ - $J$  coupling and local-field effects demonstrate the polarization splitting depending on the symmetry of the isoelectronic center.

DOI: [10.1103/PhysRevB.77.193102](https://doi.org/10.1103/PhysRevB.77.193102)

PACS number(s): 71.35.Ji, 71.55.Eq, 71.70.Gm, 78.55.Cr

Nitrogen (N) has a strong electronegativity and creates isoelectronic centers in III-V semiconductors such as GaAs and GaP. The electronic states created by the N-related centers cause substantial localization of excitons. Incorporation of a small amount of N atoms leads to dramatic changes in the local electronic structure of the host semiconductor.<sup>1,2</sup> In the impurity limit, the localized electronic states relating to N pairs and N clusters have been observed to show resolution-limited luminescence lines.<sup>3,4</sup> The extremely narrow bandwidth luminescence has been attracting strong interest for light sources such as single photons and event-ready polarization entangled photon pairs utilized in quantum information processing. From the same point of view, the atomlike properties of single self-assembled semiconductor quantum dots (QDs) have been widely studied.<sup>5-10</sup> However, the emission energy is difficult to control and, furthermore, the exchange interactions in the in-plane asymmetries of the QD cause a significant fine structure splitting of the intermediate exciton states, which eventually gives rise to the so-called “which path” information.<sup>9</sup> In contrast to the self-assembled QDs, utilization of the impurity states in semiconductor materials can achieve a narrow bandwidth bound exciton emission with defined photon energy. Recently, each individual bound exciton has been demonstrated to be able to generate single photons.<sup>11-13</sup> Since the fine structure splitting of the impurity center is influenced by the electron-hole exchange interactions and the symmetry, understanding of the detailed structure of the polarization splitting and the interactions in the center is indispensable to control the fine structure.

Here, we have studied the fine structure polarization splitting of exciton emission lines related to N pairs in GaAs. The in-plane Zeeman interaction causes a field evolution of the split states. To understand detailed exchange interactions in the centers, we performed calculations of the optical selection characteristics considering both the  $J$ - $J$  coupling and local-field effects.

N atomic-layer doped GaAs has been grown on an undoped GaAs(001) substrate by molecular-beam epitaxy. Before doping N, a 380-nm-thick GaAs-buffer layer was grown at 565 °C. The As partial pressure was  $3.0 \times 10^{-6}$  Torr. We used active nitrogen species created in a radio-frequency

plasma source from ultrapure  $N_2$  gas. The gas-flow rate was 1.0 ccm. The N doping has been performed at 570 °C on the GaAs buffer layer by confirming the N-stabilized  $(3 \times 3)$  long-range ordered surface.<sup>4,14</sup> During the N doping, the As shutter was not closed. Following the nitridation, a 50-nm-thick GaAs capping layer was grown. The sheet concentration of the doped N analyzed by secondary ion mass spectroscopy is about  $3 \times 10^{12} \text{ cm}^{-2}$ .

Photoluminescence (PL) has been performed to study exciton fine structures of isoelectronic centers in the GaAs:N sample. The excitation has been done by the 488 nm line of an argon-ion laser. The sample was set in a superconducting-magnet system at 2.5 K in a He-gas flow cooling system. PL was dispersed in a 550 mm single monochromator and detected by a liquid-nitrogen cooled silicon charge coupled device array. The resolution limit of our system is 0.1 meV.

Figure 1(a) is a typical PL spectrum of the GaAs:N sample. The spectrum shows two narrow signals at 1.4431

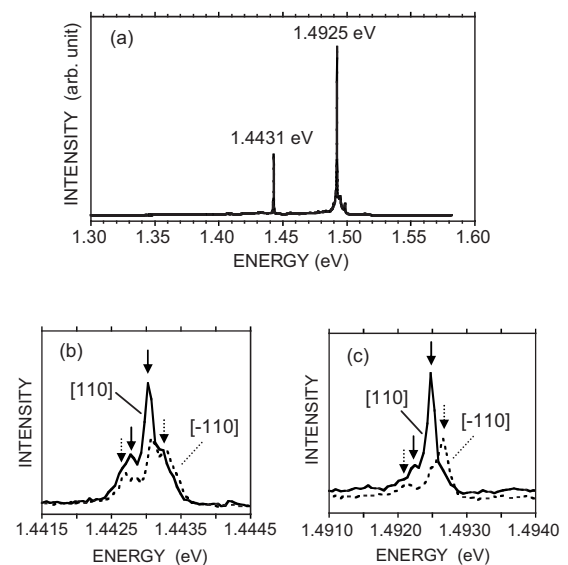


FIG. 1. (a) Typical PL spectrum of the GaAs:N sample. The fine structure polarization splittings for the 1.4431 and 1.4925 eV signals are displayed in (b) and (c), respectively.

and 1.4925 eV. This is a typical feature of the sample grown by the above mentioned atomically controlled technique, where the atomic-layer doping selects the N pairs in the (001) plane.<sup>4</sup> Figures 1(b) and 1(c) show highly resolved linearly polarized PL spectra for the 1.4431 and 1.4925 eV signals, respectively. The PL spectra exhibit clear fine structure polarization splitting. The structure consists of four lines as indicated by arrows.<sup>4,15</sup> Each spectral linewidth is close to our resolution limit. The  $[110]$  ( $[\bar{1}10]$ ) polarization corresponds to the direction showing the PL-intensity maximum (minimum). The in-plane polarization dependence reveals the twofold rotation symmetry of the emission center, which suggests a  $C_{2v}$  symmetry about its central  $[001]$  axis.<sup>4</sup> Furthermore, the PL-intensity maximum at the  $[110]$  polarization indicates that the N pair is oriented along the  $[110]$ . The  $[110]$  ( $[\bar{1}10]$ ) polarization selects the inner (outer) pair. The polarization selection of the 1.4925 eV signal is obvious as compared to that of the 1.4431 eV signal. This point will be discussed later.

We performed PL measurements in the in-plane magnetic field. The applied magnetic field direction is  $[\bar{1}10]$  which is perpendicular to the N pair direction. With increasing the magnetic field, the polarized spectra show dramatic changes depending on the polarization direction. Figures 2(a) and 2(b) display the results for the 1.4431 eV signal. The spectrum in the magnetic field splits into many signals. Similar changes can be confirmed for the 1.4925 eV signal, as shown in Figs. 2(c) and 2(d). These field evolutions indicate that the optical selection characteristics are broken by the magnetic field. As will be discussed later, the  $J$ - $J$  coupling in a biaxial field,  $C_{2v}$ , splits the  $\Gamma_6 \times \Gamma_8$  excitonic state into eight singlet states,<sup>15,16</sup> in which two transitions from the  $J=2$  to the  $J=0$  ground state are forbidden. Then, six transitions are optically allowed. Furthermore, since the polarization directions of two transitions from the  $J=1$  and 2 to the  $J=0$

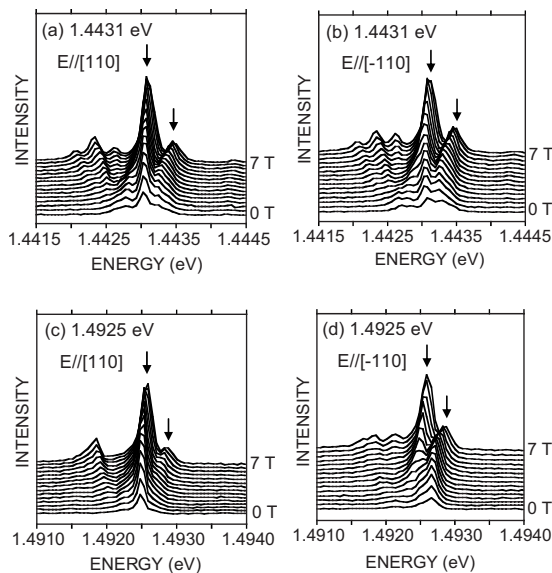


FIG. 2. Polarized magneto-PL spectra measured in the Voigt configuration. The magnetic field was applied along the  $[\bar{1}10]$  direction that is perpendicular to the N pair direction.

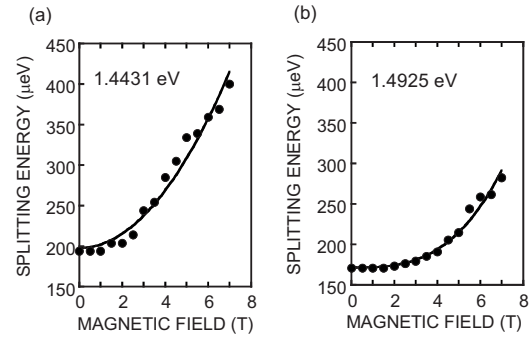


FIG. 3. Magnetic field dependence of the splitting energy indicated in Fig. 2. Solid lines indicate the quadratic dependences. The magnetic field was applied along the  $[\bar{1}10]$  direction.

ground state are parallel to the  $[001]$ , emissions due to these transitions cannot be observed when detecting PL from the (001) face. Therefore, the remaining four transitions are observed. The observed signals in Fig. 1 are attributed to these transitions. On the other hand, many more signals can be confirmed in the magneto-PL spectra displayed in Fig. 2 especially for the 1.4431 eV signal. When the magnetic field is parallel to the  $[\bar{1}10]$  direction, the  $C_{2v}$  symmetry should be preserved. Therefore, the appearance of the signals more than four lines in the high magnetic field is due to lowering

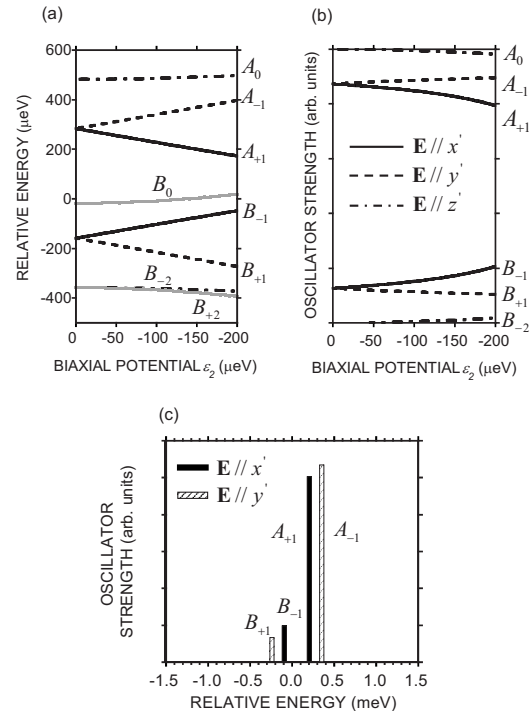


FIG. 4. Calculated (a) exciton fine structure splitting and (b) the oscillator strengths as a function of the biaxial potential  $\epsilon_2$  by using parameters of  $\gamma=1.0$  meV and  $\epsilon_1=300$   $\mu$ eV, where  $\gamma$  is the  $J$ - $J$  coupling energy and  $\epsilon_1$  and  $\epsilon_2$  are uniaxial and biaxial potentials, respectively. (c) shows typical calculated oscillator strengths by using parameters of  $\gamma=500$   $\mu$ eV,  $\epsilon_1=-170$   $\mu$ eV, and  $\epsilon_2=-130$   $\mu$ eV. In this calculation, we do not consider the quantum size effects causing the significant anisotropic polarization dependence of the oscillator strength, as shown in Fig. 1.

the symmetry of the emission center, which is considered to be caused by applying the in-plane magnetic field along an unideal direction slightly deviated from  $[\bar{1}10]$ . In a general field less than  $C_{2v}$ , six of the eight transitions become observable.

Here, we note the dominant two lines indicated by arrows in Fig. 2. The splitting energy of these peaks increases with the magnetic field. The field dependences for the 1.4431 and 1.4925 eV signals are summarized in Fig. 3. Both the results obey quadratic dependences as drawn by solid lines. The quadratic dependence is a typical feature of the bright exciton splitting caused by the in-plane Zeeman interactions.<sup>5,10</sup> Therefore, these two originate from the hybridized states of the  $|+1\rangle$  and  $|-1\rangle$  exciton states. The remarkable splitting observed in the 1.4431 eV signal demonstrates a strong long-range exchange interaction caused by tight binding of the exciton states at the N pair center.

Next, we performed theoretical calculations of the exciton fine structure of the N pairs in GaAs by considering both the  $J$ - $J$  coupling and local-field effects.<sup>16</sup> In the  $J$ - $J$  coupling

description, the exchange interaction splits the  $\Gamma_6 \times \Gamma_8$  excitonic state into a  $J=1$  triplet of energy  $E_0 + 5\gamma/8$  and a  $J=2$  quintet of energy  $E_0 - 3\gamma/8$ , where  $E_0$  is the exciton energy without the exchange interaction and  $\gamma$  is the  $J$ - $J$  coupling energy. On the other hand, the local potential with the  $C_{2v}$  symmetry couples  $x'$ ,  $y'$ , and  $z'$  eigenstates. Here, we choose that the  $x'$ ,  $y'$ , and  $z'$  axes correspond to  $[110]$ ,  $[\bar{1}10]$ , and  $[001]$ , respectively. Therefore, we need two parameters as follows:

$$\begin{array}{c|ccc} & |x'\rangle & |y'\rangle & |z'\rangle \\ \hline \langle x'| & -\epsilon_1 + \epsilon_2 & 0 & 0 \\ \langle y'| & 0 & -\epsilon_1 - \epsilon_2 & 0 \\ \langle z'| & 0 & 0 & +2\epsilon_1 \end{array}, \quad (1)$$

where  $\epsilon_1$  and  $\epsilon_2$  are uniaxial and biaxial potentials, respectively.<sup>16</sup> The energy levels and those oscillator strengths are calculated by diagonalizing the following  $8 \times 8$  matrix in the  $|J, M_J\rangle$  representation,<sup>16</sup>

$$\hat{H}_{JJ} = \begin{pmatrix} -\frac{3\gamma}{8} + \epsilon_1 & \frac{\epsilon_2}{\sqrt{6}} & -\frac{\epsilon_2}{\sqrt{6}} & 0 & 0 & 0 & 0 & 0 \\ \frac{\epsilon_2}{\sqrt{6}} & -\frac{3\gamma}{8} - \epsilon_1 & 0 & \frac{\epsilon_2}{\sqrt{6}} & 0 & 0 & 0 & 0 \\ -\frac{\epsilon_2}{\sqrt{6}} & 0 & \frac{5\gamma}{8} - \epsilon_1 & \frac{\epsilon_2}{\sqrt{6}} & 0 & 0 & 0 & 0 \\ 0 & \frac{\epsilon_2}{\sqrt{6}} & \frac{\epsilon_2}{\sqrt{6}} & -\frac{3\gamma}{8} + \epsilon_1 & 0 & 0 & 0 & 0 \\ 0 & 0 & 0 & 0 & -\frac{3\gamma}{8} - \frac{\epsilon_1}{2} & \frac{\epsilon_1\sqrt{3}}{2} & -\frac{\epsilon_2}{2\sqrt{3}} & \frac{\epsilon_2}{2} \\ 0 & 0 & 0 & 0 & \frac{\epsilon_1\sqrt{3}}{2} & \frac{5\gamma}{8} + \frac{\epsilon_1}{2} & \frac{\epsilon_2}{2} & \frac{\epsilon_2}{2\sqrt{3}} \\ 0 & 0 & 0 & 0 & -\frac{\epsilon_2}{2\sqrt{3}} & \frac{\epsilon_2}{2} & \frac{5\gamma}{8} + \frac{\epsilon_1}{2} & -\frac{\epsilon_1\sqrt{3}}{2} \\ 0 & 0 & 0 & 0 & \frac{\epsilon_2}{2} & \frac{\epsilon_2}{2\sqrt{3}} & -\frac{\epsilon_1\sqrt{3}}{2} & -\frac{3\gamma}{8} - \frac{\epsilon_1}{2} \end{pmatrix}. \quad (2)$$

Figure 4(a) shows a calculated splitting pattern of the exciton levels as a function of the biaxial potential  $\epsilon_2$  with using parameters of  $\gamma=500 \mu\text{eV}$  and  $\epsilon_1=-170 \mu\text{eV}$ . Here,  $A$  and  $B$  represent the triplet and quintet states, respectively. The indices of  $A$  and  $B$  indicate the value of  $M_J$ . The biaxial local field splits all degenerate energy levels. Figure 4(b) shows the calculated oscillator strengths of the energy levels shown in Fig. 4(a). Solid, dashed, and dash-dotted lines indicate the polarized components along the  $x'$ ,  $y'$ , and  $z'$  directions, respectively. Only two levels,  $B_0$  and  $B_{+2}$ , remain

dipole forbidden transitions, while it is noted that six levels become dipole allowed transitions in the  $C_{2v}$  symmetry. In our experimental configuration, the  $x'$  and  $y'$  polarization components can be observed. Figure 4(c) shows a typical calculated oscillator strengths by using parameters of  $\gamma=500 \mu\text{eV}$ ,  $\epsilon_1=-170 \mu\text{eV}$ , and  $\epsilon_2=-130 \mu\text{eV}$ . In this calculation, we do not consider the quantum size effects causing the significant anisotropic polarization dependence of the oscillator strength, as shown in Fig. 1. Filled and hatched boxes indicate the polarized components along the  $x'$  and  $y'$  direc-

tions, respectively. The calculated result reproduces the observed optical selection characteristics; the  $x'(y')$  polarization selects the inner (outer) pair, and the oscillator strength of the high energy level is larger than that of the low energy level for each polarization. According to these results, it is concluded that the exciton fine structure can be analyzed by the local-field effects in the  $C_{2v}$  symmetry based on the  $J$ - $J$  coupling representation. On the other hand, the fine structure polarization splitting of the 1.4431 eV signal is rather unclear than that of the 1.4925 eV signal, which never appears in the ideal  $C_{2v}$  symmetry. We need to consider local-field effects in a lower symmetry than  $C_{2v}$  for the 1.4431 eV center.

In summary, we have studied the fine structure polariza-

tion splitting of exciton emission lines related to N pairs formed in GaAs. The localized bound excitons consist of four signals, which can be selected by linear polarization. In the in-plane magnetic field, the Zeeman interaction causes a quadratic dependence of the bright exciton splitting. The theoretical calculations of the optical selection characteristics demonstrate the polarization splitting depending on the symmetry of the isoelectronic center when considering substantial  $J$ - $J$  coupling and the strong biaxial field.

This work was supported in part by the Scientific Research Grant-in-Aid from the Ministry of Education, Culture, Sports, Science and Technology (Contracts No. 19360146 and No. 20045011).

---

\*kita@eedept.kobe-u.ac.jp

<sup>1</sup>W. Shan, W. Walukiewicz, J. W. Ager III, E. E. Haller, J. F. Geisz, D. J. Friedman, J. M. Olson, and S. R. Kurtz, Phys. Rev. Lett. **82**, 1221 (1999).

<sup>2</sup>P. R. C. Kent and A. Zunger, Phys. Rev. B **64**, 115208 (2001).

<sup>3</sup>T. Makimoto and N. Kobayashi, Appl. Phys. Lett. **67**, 688 (1995).

<sup>4</sup>T. Kita and O. Wada, Phys. Rev. B **74**, 035213 (2006).

<sup>5</sup>M. Bayer, O. Stern, A. Kuther, and A. Forchel, Phys. Rev. B **61**, 7273 (2000).

<sup>6</sup>M. Bayer, G. Ortner, O. Stern, A. Kuther, A. A. Gorbunov, A. Forchel, P. Hawrylak, S. Fafard, K. Hinzer, T. L. Reinecke, S. N. Walck, J. P. Reithmaier, F. Klopff, and F. Schäfer, Phys. Rev. B **65**, 195315 (2002).

<sup>7</sup>C. Santori, M. Pelton, G. Solomon, Y. Dale, and Y. Yamamoto, Phys. Rev. Lett. **86**, 1502 (2001).

<sup>8</sup>Z. Yuan, B. E. Kardynal, R. M. Stevenson, A. J. Shield, C. L. Lobo, K. Cooper, N. S. Beattie, D. A. Ritchie, and M. Pepper, Nature (London) **295**, 102 (2002).

<sup>9</sup>R. M. Stevenson, R. J. Young, P. Atkinson, K. Cooper, D. A. Ritchie, and A. J. Shield, Nature (London) **439**, 179 (2006).

<sup>10</sup>R. M. Stevenson, R. J. Young, P. See, D. G. Gevaux, K. Cooper, P. Atkinson, I. Farrer, D. A. Ritchie, and A. J. Shields, Phys. Rev. B **73**, 033306 (2006).

<sup>11</sup>C. Kurtsiefer, S. Mayer, P. Zarda, and H. Weinfurter, Phys. Rev. Lett. **85**, 290 (2000).

<sup>12</sup>S. Strauf, P. Michler, M. Klude, D. Hommel, G. Bacher, and A. Forchel, Phys. Rev. Lett. **89**, 177403 (2002).

<sup>13</sup>M. Ikezawa, Y. Sakuma, and Y. Masumoto, Jpn. J. Appl. Phys., Part 2 **36**, L871 (2007).

<sup>14</sup>N. Shimizu, T. Inoue, T. Kita, and O. Wada, J. Cryst. Growth **301-302**, 34 (2007).

<sup>15</sup>S. Francoeur, J. F. Klem, and A. Mascarenhas, Phys. Rev. Lett. **93**, 067403 (2004).

<sup>16</sup>B. Gil, J. Camassel, P. Merle, and H. Mathieu, Phys. Rev. B **25**, 3987 (1982).